Ab Initio Study of the Insertions of Methylene and Silylene into Methane, Silane, and Hydrogen

Mark S. Gordon*† and David R. Gano‡

Contribution from the Department of Chemistry, North Dakota State University, Fargo, North Dakota 58105, and Department of Chemistry, Minot State College, Minot, North Dakota 58701. *Received November 28, 1983*

Abstract: The transition states for several insertion reactions have been determined at the 3-21G level of theory. While the insertions of CH_2 and SiH_2 into the CH and SiH bonds of methane and silane, respectively, all have nonzero SCF barriers, only the insertion of silylene into methane retains a nonzero barrier when third-order Møller–Plesset perturbation theory corrections are included with the 6-31G* basis set. The intrinsic reaction coordinates for the carbene and silylene insertions into methane are used to provide a pictorial view of these reactions and to relate the calculations to earlier studies. The insertion of silylene into H_2 is analyzed at higher levels of theory in order to consider the relative importance of improved basis sets, multiconfigurational wave functions, and large-scale configuration interaction on the calculated barrier.

I. Introduction

The insertion of methylene into H–H and C–H bonds has been the subject of several theoretical papers over the past 10 years.[1-6] On the basis of the results of these studies, it is apparent that the insertions occur in a concerted, non-least-motion manner with little or no barrier. Furthermore, it has been suggested[4,6] that the reactions occur in two stages: an "electrophilic" step in which the empty p orbital on the methylene carbon attacks the H–Y bond to form a three-center bond, followed by a "nucleophilic"

PHASE 1: ELECTROPHILIC

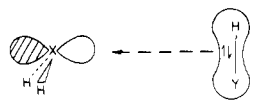

step corresponding to the interaction between the methylene lone pair and the H–Y antibonding molecular oribital. Hoffmann

PHASE 2: NUCLEOPHILIC

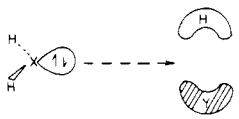

and co-workers[1] have proposed that the initial approach is "abstraction-like", with the X–H–Y bond nearly collinear until just after the transition state. More recent calculations[3-6] suggest a more rapid formation of a three-center bond in the $CH_2 + H_2$ reaction.

Experiment[7,8] and theory appear to be in agreement regarding the lack of a significant barrier in the $CH_2 + H_2$ reaction. Similarly, recent ab initio calculations including perturbation theory[9] and configuration interaction[10] corrections to the Hartree–Fock wave functions find a small but nonzero barrier to the insertion of silylene (SiH_2) into the H–H bond. Here again, theory is in agreement with the 5–6 kcal/mol activation energy observed for the reaction by John and Purnell.[11]

To date, ab initio calculations have been limited to the insertions into H_2. For CH_2, one expects[12] insertions into other Y–H bonds to be equally facile. On the other hand, it has recently been determined[13] that the insertion of SiH_2 into C–H occurs with an even larger activation energy than that observed for the $SiH_2 + H_2$ reaction. Insertions of both carbene and silylene into Si–H appear to be barrier free.[13] In order to compare the carbene and silylene insertions, the following four reactions have been studied with ab initio wave functions, including corrections for electron correlation:

$$:CH_2 + CH_4 \rightarrow C_2H_6 \quad (1)$$

$$:CH_2 + SiH_4 \rightarrow SiH_3CH_3 \quad (2)$$

$$:SiH_2 + CH_4 \rightarrow SiH_3CH_3 \quad (3)$$

$$:SiH_2 + SiH_4 \rightarrow Si_2H_6 \quad (4)$$

In addition, the $SiH_2 + H_2$ insertion reaction is used as a probe of the effect of increasing sophistication of the calculation.

Table I. Energetics for Insertion Reactions (kcal/mol)

	E_b[a]			
	SCF		MP3/6-31G*//3-21G	
reaction	3-21G	6-31G*		ΔE (ΔH_0)[b]
$SiH_2 + H\text{–}CH_3$	45.3	43.1	27.5 (17–19)	−49.0 (−49.9)
$SiH_2 + H\text{–}SiH_3$	15.8		0 (~0)	−54.5 (−45.2)
$CH_2 + H\text{–}CH_3$	9.1	9.1	0 (0)	−115.6 (−102.2)
$CH_2 + H\text{–}SiH_3$	2.1		0 (0)	−125.1 (−120.0)

[a] Calculated barrier heights, excluding zero point energy. Experimental values are given in parentheses: See ref 12, 13. [b] Overall reaction exothermicities. Calculated values are from MP3/6-31G*//3-21G. Experimental values given in parentheses. For SiH_2, see ref 11. For CH_2, see: Kollmar, H.; Staemmler, V. *Theor. Chim. Acta* **1979**, *51*, 207. For methylsilane, see: O'Neal, H. E.; Ring, M. A. *J. Organomet. Chem.* **1981**, *213*, 419. For remaining compounds, see: NBS Technical Note 270-73, US Government Printing Office, Washington, DC, 1968.

† North Dakota State University.
‡ Minot State College.

(1) Dobson, R. C.; Hayes, D. M.; Hoffmann, R. *J. Am. Chem. Soc.* **1971**, *93*, 6188.
(2) Kollmar, H. *Tetrahedron* **1972**, *28*, 5893.
(3) Bauschlicher, C. W.; Haber, K.; Schaeffer, H. F., III; Bender, C. F. *J. Am. Chem. Soc.* **1977**, *99*, 3610.
(4) Kollmar H. *J. Am. Chem. Soc.* **1978**, *100*, 2660.
(5) Kollmar, H.; Staemmler, V. *Theor. Chim. Acta.* **1979**, *51*, 207.
(6) Jeziorek, D.; Zurawski, B. *Int. J. Quantum Chem.* **1979**, *16*, 277.
(7) Jones, M.; Moss, R. A. "Carbenes"; Wiley: New York, 1972 and 1975; Vol. I and II.
(8) Kirmse, W. "Carbene Chemistry"; Academic Press: New York, 1971.
(9) Gordon, M. S. *J. Chem. Soc., Chem. Commun.* **1981**, 890.
(10) Grev, R. S.; Schaeffer, H. F., III *J. Chem. Soc., Chem Commun.* **1983**, 785.
(11) John. P.; Purnell, J. H. *J. Chem. Soc., Faraday Trans. B, 1* **1973**, *69*, 1455.
(12) Sawrey, B. A.; O'Neal, H. E.; Ring, M. A.; Coffey, D. *Int. J. Chem. Kinet.*, **1984**, *16*, 31.
(13) Davidson, I. M. T.; Lawrence, F. T.; Ostah, N. A. *J. Chem. Soc., Chem. Commun.* **1980**, 659.

0002-7863/84/1506-5421$01.50/0

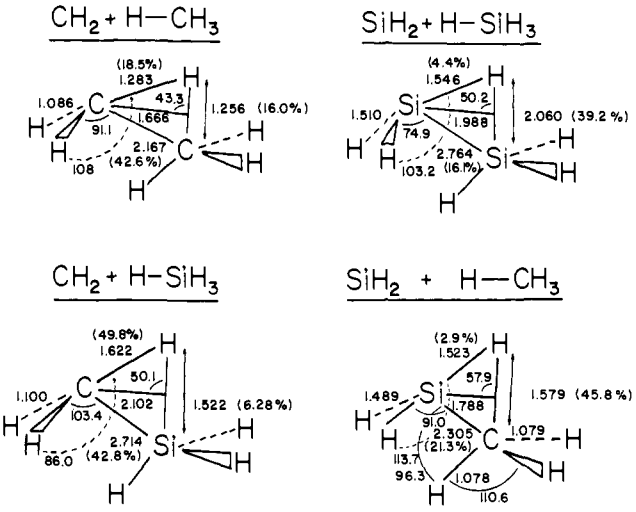

Figure 1. Transition-state structures. Bond lengths in Å, angles in deg.

II. Computational Approach

Searches for transition states were carried out using the Schlegel algorithm[14] contained in GAUSSIAN80.[15] Since we have found it to be very effective at providing initial guesses at saddle points, the minimal STO-2G basis set[16] was used for this purpose for all four molecules, at the SCF level of approximation. The structures so obtained were then refined with the split-valence 3-21G basis set.[17] Two of the reactions, 1 and 3, have been probed in some detail by determining the intrinsic reaction coordinate (IRC)[18] and obtaining Boys localized molecular orbitals[19] along the two reaction paths. For these two reactions, the transition-state structures were further refined at the 6-31G*[20] SCF level. Finally, all stationary points and selected points along the IRC's for reactions 1 and 3 were improved by adding third-order perturbation (MP3)[21] corrections to the Hartree–Fock energies, and molecular orbital contour plots were drawn by using the ALIS network of programs.[22]

III. Results and Discussion

The 3-21G SCF transition-state structures for reactions 1–4 are displayed in Figure 1, and the corresponding pertinent energetics are listed in Table I. Despite the fact that all but one of the barriers disappears upon the introduction of correlation corrections, some useful information can be gleaned from these structures. Given in parentheses in Figure 1 is the percent increase in the substrate Y–H distance at the transition state relative to the value at separated reactants. At the SCF level, this percentage is largest for the reaction with the largest calculated barrier ($SiH_2 + CH_4$) and decreases steadily with decreasing barrier height. Thus, the smaller barriers, and those that disappear at the higher computational level, occur progressively earlier in the reaction channel. Qualitatively, this is also consistent with the increasing magnitude of the overall energy differences (ΔE in Table I) for these reactions and with the Hammond postulate.[23] Also shown in Figure 1 is the increase in each of the newly forming bonds relative to the bond lengths in the final products. The percent increase in the forming X–H bond is consistent with the foregoing discussion, while there is no clear trend for the X–Y bond.

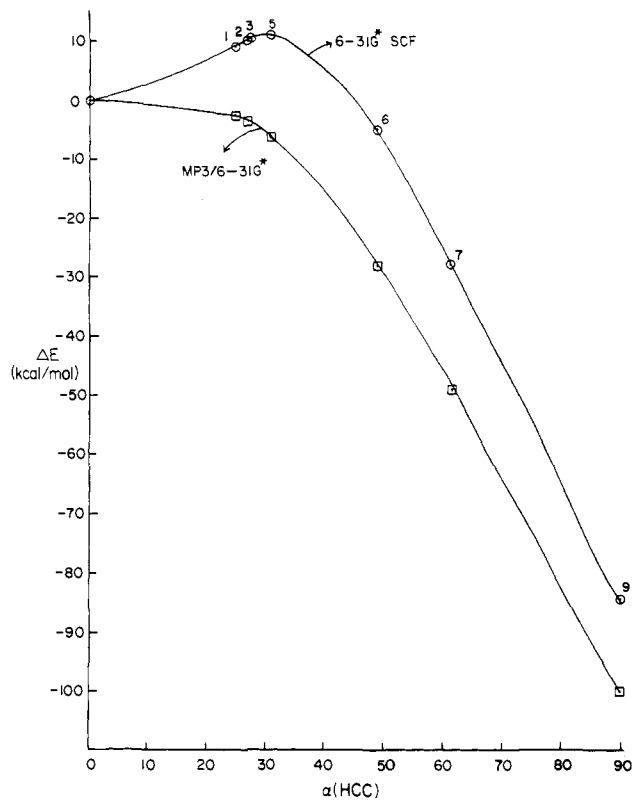

Figure 2. Energies along the IRC for $CH_2 + CH_4 \rightarrow C_2H_6$.

For reactions 1 and 3, the transition-state structures shown in Figure 1 have been reevaluated using 6-31G* SCF wave functions. As expected, the resultant structures differ from their 3-21G counterparts primarily in a shortening of the three bonds involved in the reaction: The X–H, X–Y, and Y–H bonds are 1.502, 2.257, and 1.547 Å, respectively, for the $SiH_2 + CH_4$ reaction. The corresponding bond lengths for the $CH_2 + CH_4$ reaction are 1.275, 2.135, and 1.226 Å, respectively. As shown in Table I, these bond length shortenings have only a small effect on the calculated SCF barriers, so subsequent investigations have been performed using the 3-21G structures, particularly because generation of the IRC with 6-31G* wave functions is much more time consuming. Further justification for this approach is that one expects the lengthening of these transition-state bonds due to correlation effects to be roughly canceled by the shortening due to polarization functions.[24]

The calculated MP3/6-31G*//3-21G barriers are compared in Table I with the esimated experimental activation energies of Ring, O'Neal, Davidson, and co-workers.[12,13] As noted earlier, only the $SiH_2 + CH_4$ reaction is predicted to have a nonzero barrier at this level of computation. This is in agreement with experiment, although the calculated barrier is somewhat too high. The calculated thermodynamic ΔE's are generally within 10% of their corresponding experimental estimates. Note also that the calculations are more consistent with the silylene results of John and Purnell[11] than with those of Robertson et al.[25]

Starting from the saddle-point structure and force field, one may follow the intrinsic reaction coordinate (IRC) for the reaction forward toward products or back toward reactants, according to the prescription of Fukui[18a] and Morokuma.[18b] Both the 6-31G* SCF and MP3/6-31G* energies along the IRC are shown in Figures 2 and 3 for reactions 1 and 3, respectively. The disap-

(14) Schlegel, H. B. *J. Comput. Chem.* **1982**, *3*, 214.
(15) Binkley, J. S.; Whiteside, R. A.; Krishnan, R.; Seeger, R.; DeFrees, D. J.; Schlegel, H. B.; Topiol, S.; Kahn, L. R.; Pople, J. A. *QCPE* **1981**, *13*, 406.
(16) Collins, J. B.; Schleyer, P. v. R.; Binkley, J. S.; Pople, J. A. *J. Chem. Phys.* **1976**, *64*, 5142.
(17) Binkley, J. S.; Pople, J. A.; Hehre, W. J. *J. Am. Chem. Soc.* **1980**, *102*, 939. Gordon, M. S.; Binkley, J. S.; Pople, J. A.; Pietro, W. J.; Hehre, W. J. *J. Am. Chem. Soc.* **1982**, *104*, 2797.
(18) (a) Fukui, K. *J. Phys. Chem.* **1970**, *74*, 4161. (b) Ishida, K.; Morokuma, K.; Komornicki, A. *J. Chem. Phys.* **1977**, *66*, 2153.
(19) Foster, J. M.; Boys, S. F. *Rev. Mod. Phys.* **1963**, *32*, 300.
(20) Francl, M. M.; Pietro, W. J.; Hehre, W. J.; Binkley, J. S.; Gordon, M. S.; DeFrees, D. J.; Pople, J. A. *J. Chem. Phys.* **1982**, *77*, 3654. Gordon, M. S. *Chem. Phys. Lett.* **1980**, *76*, 163.
(21) Pople, J. A.; Seeger, R.; Krishnan, R. *Int. J. Quantum Chem.* **1979**, *511*, 149.
(22) Ruedenberg, K.; Gilbert, M. M.; Schmidt, M. W., program developed at Iowa State University.
(23) Hammond, G. S. *J. Am. Chem. Soc.* **1955**, *77*, 334.
(24) DeFrees, D. J.; Levi, B. A.; Pollack, S. K.; Hehre, W. J.; Binkley, J. S.; Pople, J. A. *J. Am. Chem. Soc.* **1979**, *101*, 4085.
(25) Robertson, R.; Hils, D.; Gallagher, A. *Chem. Phys. Lett.* **1984**, *103*, 397.

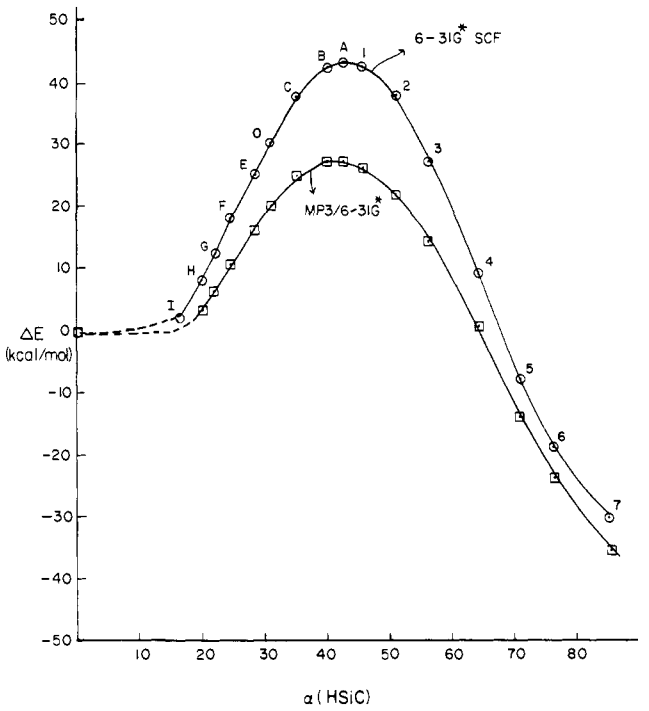

Figure 3. Energies along the IRC for $SiH_2 + CH_4 \rightarrow CH_3SiH_3$.

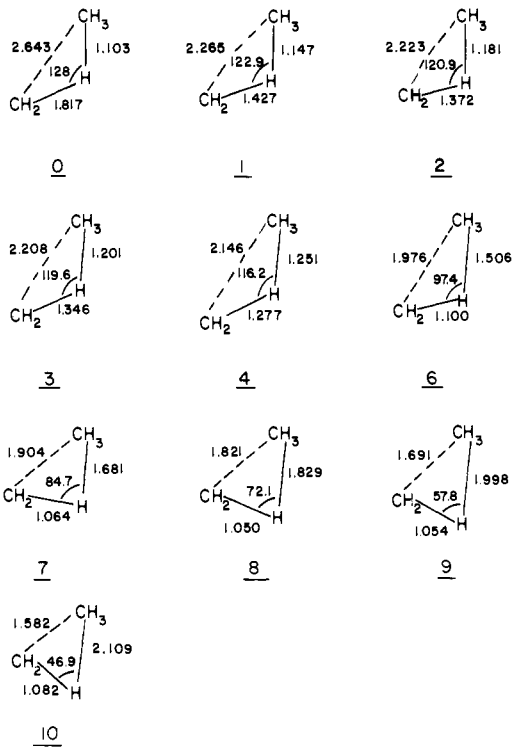

Figure 4. Geometries along the IRC for $CH_2 + CH_4 \rightarrow C_2H_6$.

pearance of the $CH_2 + CH_4$ barrier and the diminishing of the $SiH_2 + CH_4$ barrier are clearly shown in these figures. Schematics of the pertinent geometric parameters along the two IRC's are shown in Figures 4 and 5, respectively. To aid in the comparison, the points on the curves in Figures 2 and 3 are labeled in the same manner as the structures in Figures 4 and 5. Note that the initial angle of attack by XH_2 in both reactions is rather large. While this XHY angle closes down as the reactions proceed, the initial approach is qualitatively consistent with the early suggestion by Dobson, Hayes, and Hoffmann[1] that the insertion starts out looking nearly like an abstraction. The quantitative difference is that in the transition states the angles are already quite bent, particularly in the case of silylene.

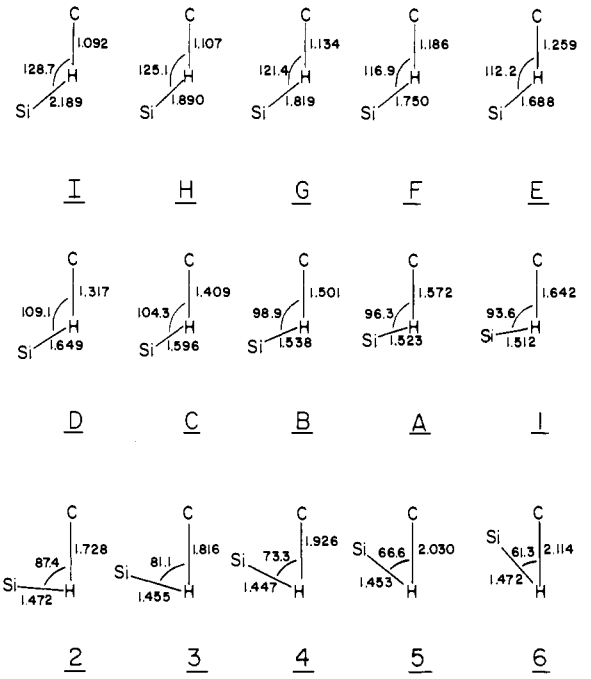

Figure 5. Geometries along the IRC for $SiH_2 + CH_4 \rightarrow CH_3SiH_3$.

Table II. Net 6-31G*//3-21G Mulliken Charges on XH_2 Fragments F and Central Atom X

X = Si			X = C		
point	q_F	q_{Si}	point	q_F	q_C
I	−0.02	0.23	0	−0.03	−0.35
H	−0.06	0.20	1	−0.13	−0.45
G	−0.06	0.18	2	−0.15	−0.47
F	−0.09	0.15	3	−0.17	−0.49
E	−0.10	0.12	4	−0.20	−0.52
D	−0.11	0.11	6	−0.22	−0.58
C	−0.10	0.10	7	−0.20	−0.56
B	−0.04	0.12	8	−0.17	−0.53
A	−0.02	0.14	9	−0.15	−0.49
1	0.03	0.17	10	−0.16	−0.48
2	0.11	0.23			
3	0.16	0.30			
4	0.24	0.40			
5	0.27	0.45			
6	0.29	0.49			
7	0.30	0.52			

The sequences of structures shown in Figures 4 and 5 are also consistent with the two-phase picture of the reaction proposed earlier,[4,6] since only in the later stages does the XH_2 fragment position itself to interact strongly as a nucleophile with the substrate Y–H antibonding MO. This is illustrated in Table II, which lists the net Mulliken charge densities on the XH_2 fragments along the respective intrinsic reaction coordinates. At the early part of the approach (points I–D in methylsilane and 0–6 in ethane) the negative charge on the approaching XH_2 fragment increases. This reflects the expected donation of electron density from the CH_4 substrate into the X lone pair during the sideways electrophilic attack. This may be seen from the concurrent electron density increase on X itself. Note also that this electrophilic phase extends deeper into the reaction path for X = C than for X = Si (point 5 is the transition state in the former). As the reaction proceeds further, the interaction of the X lone pair with the CH antibonding orbital results in electron density shifting from XH_2 to CH_4.

A further view of the progress of these reactions is provided in Figures 6 and 7, where the key Boys localized orbitals are presented for the two reactions at selected points along the respective paths. Figure 6 depicts the transformation of the X lone pair into an X–H bond, while the metamorphosis to an X–C bond from a Y–H bond via a three-center Y–H–X moiety is traced

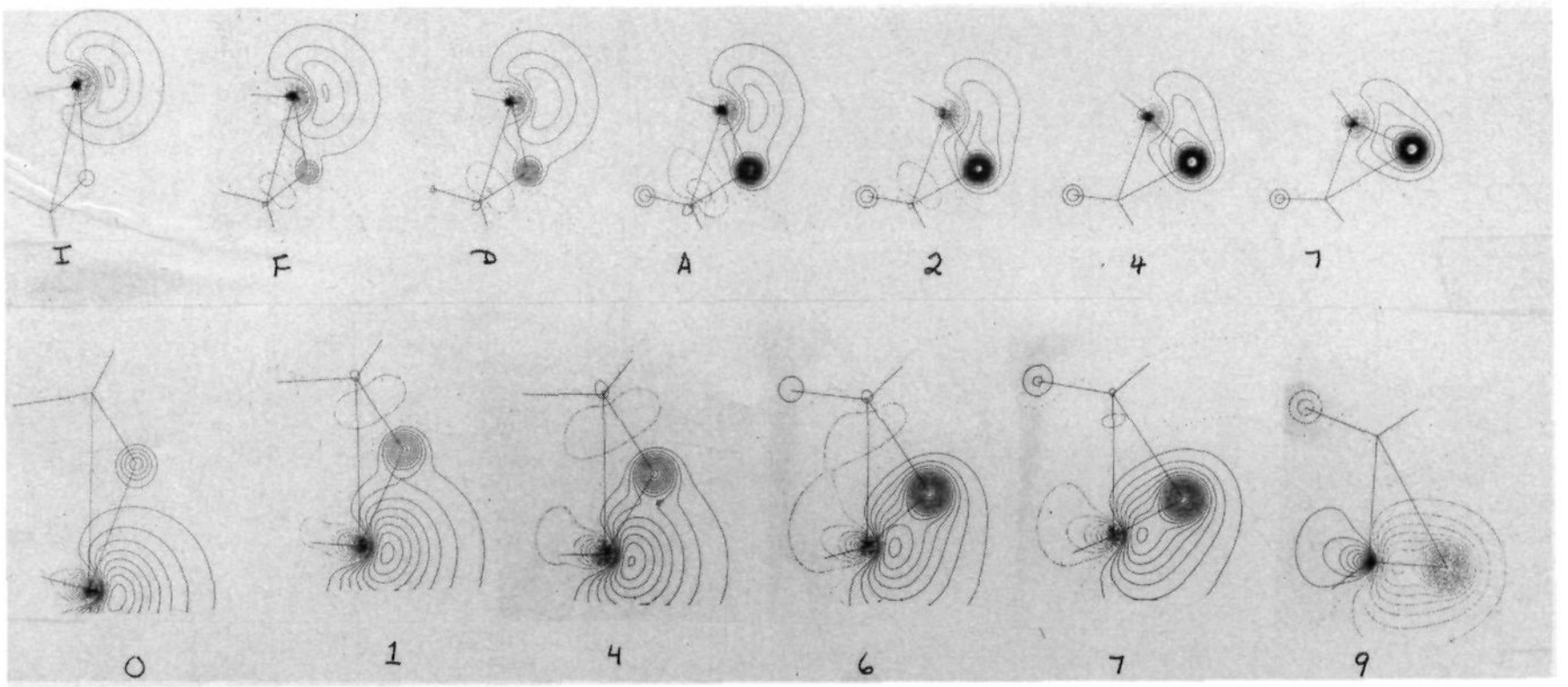

Figure 6. YH_2 lone pair → YH bond: Y = Si (top), C (bottom).

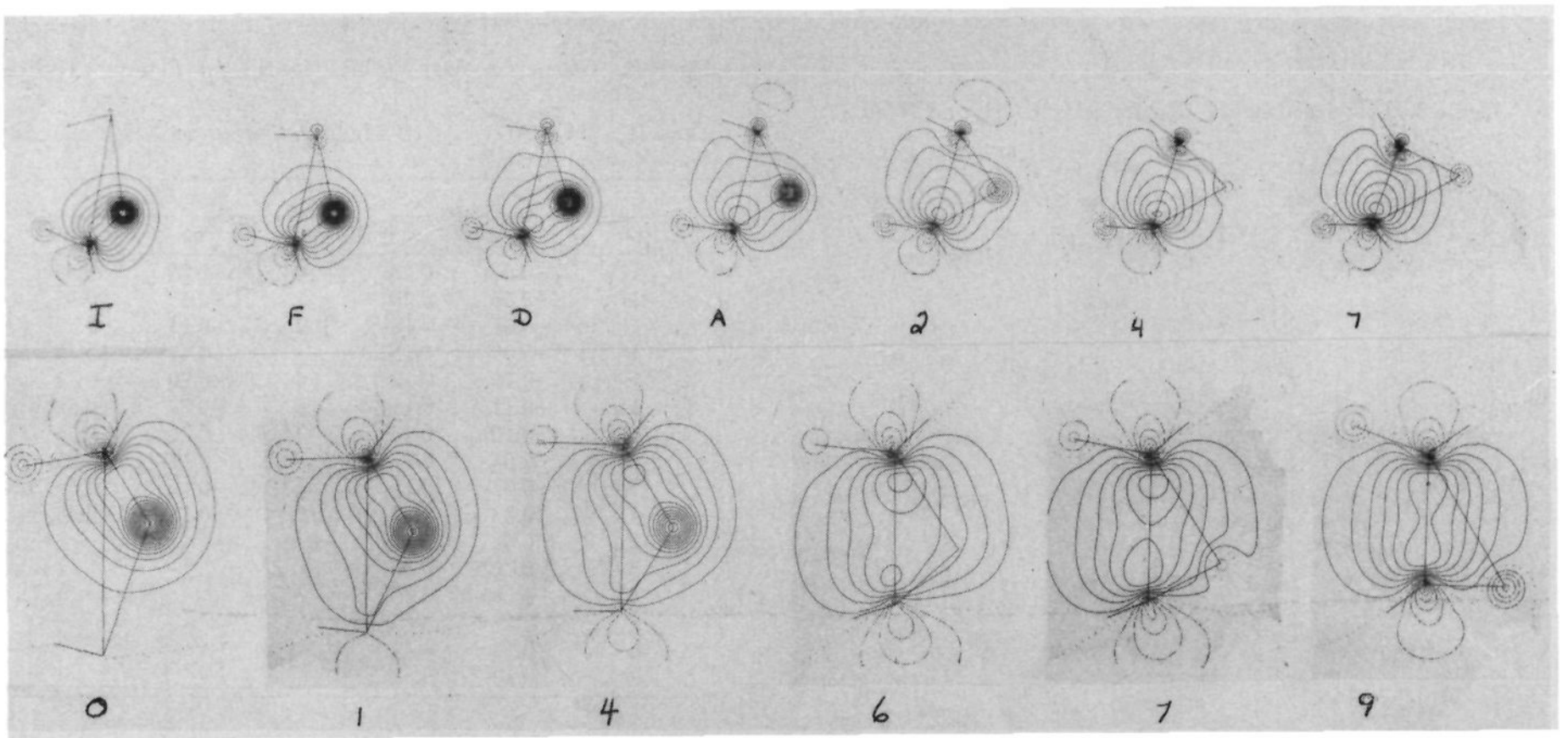

Figure 7. CH bond → CY bond: Y = Si (top), C (bottom).

in Figure 7. Particularly in the latter figure, the earlier formation of the X–C bond in the case of X = C is evident. This is consistent with the smaller SCF and vanishing MP3 barrier for X = C.

IV. Conclusions

A. Summary. The major conclusion of this work is that of the four insertion reactions considered, only the insertion of SiH_2 into a C–H bond of CH_4 has a nonzero barrier to surmount. This and the fact that the $SiH_2 + CH_4$[13] barrier is larger than that for $SiH_2 + H_2$[11] are consistent with available experimental evidence. The nonzero barriers for these reactions are probably related to their smaller thermodynamic ΔE's and to the steric requirements for inserting a bulky attacking group, SiH_2, into relatively strong bonds. Analysis of the reaction paths for the insertions of CH_2 and SiH_2 into CH_4 provides qualitative support for early speculations regarding the initial geometry of the attack and the two-phase nature of the reaction.

B. Further Considerations. One might speculate with regard to the disparity between experiment and theory for the $SiH_2 + CH_4$ insertion barrier, particularly since zero-point corrections are expected[10] to increase the computed activation energy relative to the barrier. There are three factors which may contribute to too large a theoretical barrier: (a) The basis set is incomplete, since polarization functions have not been included on the hydrogens. (b) A single configuration description may be inadequate to describe the transition state. A multiconfiguration wave function may be necessary to obtain the corresponding structure. (c) Higher levels of correlation may be needed for a proper description of the process. Since all three corrections will require considerable increments of computer time, and since point a will be most critical when the substrate is H_2 rather than Y–H, initial probes of these points have been carried out with the $SiH_2 + H_2$ reaction. Here the experimental activation energy is estimated[11] to be about 6 kcal/mol, whereas the MP3/6-31G*//3-21G barrier is 8.4 kcal/mol. Retaining the SCF geometry and adding p functions to all hydrogens (MP3/6-31G**//3-21G) reduces this barrier to 5.5 kcal/mol. This is a considerable improvement but still a bit too high since the zero-point corrections will raise the barrier to about a 7.5-kcal/mol activation energy.

The importance of a multiconfigurational description has been investigated by using HONDO/GAMESS[26] and the FORS/MCSCF

(26) Dupuis, M.; Spangler, D.; Wendoloski, J. J. NRCC Software Catalog, University of California, Berkeley, 1980, Vol. 1.

approach.[27] Since the reaction involves the formation of two new SiH bonds and the breaking of an H–H bond, the proper MCSCF description requires the inclusion of all configurations generated from the distribution of four electrons among four active orbitals. In the separated reactants, the four active orbitals correspond to the lone pair and empty p orbitals on SiH_2 and the bonding and antibonding orbitals on H_2. Relative to the SCF transition state,[9] this 20-configuration MCSCF with a 6-31G* basis set (MC-(4,4)/6-31G*) results in a small lengthening in the two forming SiH bonds (0.06 and 0.01 Å for the longer and shorter bonds, respectively) and virtually no change in the H–H distance. Grev and Schaeffer[10] (GS) have performed a two-configuration transition-state optimization for this system and obtained a similar structure. The GS H–H distance is about 0.04 shorter, probably a reflection of the incorporation of p functions into the basis set. The MP3//MC(4,4)/6-31G* barrier is found to be 5.2 kcal/mol.

At the MCSCF(4,4)/6-31G* level of computation, the calculated barrier is 16.2 kcal/mol. Addition of second-order configuration interaction (SOCI = all single and double excitations from the 20 MCSCF configurations) incorporates more than 25 000 configurations and reduces the calculated barrier to 8.4 kcal/mol. Note that this is very similar to the MP3/6-31G* result quoted above. Grev and Schaeffer have performed the analogous CI with their two-configuration wave function (~7000 configurations) and found a rather smaller barrier (4.8 kcal/mol). Again, the difference is very likely to be found in their incorporation of p functions on the hydrogens.

Since the MP3/6-31G** barrier for $SiH_2 + H_2$ appears to be fairly insensitive to geometry, a preliminary probe of the effect of hydrogen-polarization functions on the $SiH_2 + CH_4$ reaction was carried out using the geometries quoted in Figure 1. This results in a barrier of 26.8 kcal/mol. As expected, the importance of hydrogen p functions is smaller than for $SiH_2 + H_2$ and still leaves the calculated barrier well above the experimental value. The effect of using multiconfiguration wave functions on this result will be probed in a later paper.

Acknowledgment. This work was supported by the donors of the Petroleum Research Fund, administered by the American Chemical Society. The computer time made available by the North Dakota State University Computer Center is gratefully acknowledged, as are several stimulating discussions with Dr. Michael Schmidt.

Registry No. :CH_2, 2465-56-7; :SiH_2, 13825-90-6; CH_4, 74-82-8; SiH_4, 7803-62-5; H_2, 1333-74-0.

(27) Ruedenberg K.; Schmidt, M. W.; Gilbert, M. M.; Elbert, S. T. *Chem. Phys.* **1982**, *71*, 48.

Thermodynamic and Structural Aspects on Liquid and Solid Benzene. Monte Carlo Study

Per Linse

Contribution from Physical Chemistry 1, Chemical Center, S-220 07 LUND, Sweden.
Received December 12, 1983

Abstract: Liquid and solid benzene have been examined by Monte Carlo simulations using pairwise additive potentials obtained from ab initio quantum chemical calculations. Various experimental data are satisfactorily reproduced by this potential, which generally is an improvement of empirical ones. In the liquid, in comparison with the solid phase, there is almost no angular orientation correlation between pairs of molecules except at very short distances, where the non-spherical exchange repulsion favors the stacked configuration. However, the repulsive quadrupole–quadrupole interaction strongly reduces the probability of the stacked configuration at such short separations. In solid benzene at 258 K, the effective rotational energy barrier is smaller for rotation around the C_6 axis than for rotation around a C_2 axis. The relatively large freedom of rotation around the C_6 axis smooths the otherwise oscillated structure of the atom–atom distribution functions.

I. Introduction

Computer simulations may provide data on structural and dynamic properties of liquids. Liquid benzene has been the subject of several investigations[1-3] by simulation techniques using empirical pair potentials based on site–site interactions. Evans and Watts have investigated several benzene–benzene potentials[4,5] and have used a six-site Lennard–Jones potential to calculate static properties using the Monte Carlo (MC) technique.[1] Steinhauser[2] has reported both structural and dynamic results from molecular dynamics (MD) calculations based on the same potential as in the MC work of Evans and Watts. Claessens et al.[3] showed that an additional point quadrupole, fixed to its experimental value, at the center of the benzene molecule might improve the empirical potential by reducing the probability of the stacked configuration.

This work presents a MC study of liquid and solid benzene based on an ab initio quantum mechanical pair potential.[6] Dynamic aspects on benzene will be deferred to a second paper.

II. Benzene Pair Potentials

The benzene potential used in the present simulations has been described by Karlström et al.[6] It was obtained from ab initio quantum chemical calculations using the Hartree–Fock self-consistent-field (HF-SCF) approximation, and the dispersion energy was obtained by a perturbation procedure. The resulting intermolecular energy function is a linear combination of atom–atom terms of the form

$$E = \sum_i \left[A_i \frac{1}{r_i} + B_i \frac{1}{r_i^4} + C_i \frac{1}{r_i^6} + D_i \frac{1}{r_i^9} + E_i \frac{1}{r_i^{12}} \right] \quad (1)$$

where i sums over the interatomic distances C–C, C–H, and H–H. Table I gives the benzene geometry used and the coefficients for the best fit.

The same quantum chemical data have been used to obtain the best Lennard–Jones (LJ) parameters for four potentials with the same fitting procedure was earlier.[6] Table II shows the potentials, their mean-square deviation, and best LJ parameters with their standard deviations. An analysis of the potentials for different configurations shows that potential 1 is incapable of simultaneously

(1) Evans, D. J.; Watts, R. O. *Mol. Phys.* **1976**, *32*, 93.
(2) Steinhauser, O. *Chem. Phys.* **1982**, *73*, 155.
(3) Claessens, M.; Ferrario, M.; Ryckaert, J.-P. *Mol. Phys.* **1983**, *50*, 217.
(4) Evans, D. J.; Watts, R. O. *Mol. Phys.* **1975**, *29*, 777.
(5) Evans, D. J.; Watts, R. O. *Mol. Phys.* **1976**, *31*, 83.
(6) Karlström, G.; Linse, P.; Wallqvist, A.; Jönsson, B. *J. Am. Chem. Soc.* **1983**, *105*, 3777.

0002-7863/84/1506-5425$01.50/0